

Building and evaluation of a PBPK model for inulin in rats

Version	1.0-OSP11.3
based on <i>Model Snapshot and Evaluation Plan</i>	https://github.com/Open-Systems-Pharmacology/Inulin-Model/releases/tag/v1.0
OSP Version	11.3
Qualification Framework Version	3.2

This evaluation report and the corresponding PK-Sim project file are filed at:

<https://github.com/Open-Systems-Pharmacology/OSP-PBPK-Model-Library/>

Table of Contents

- 1 Introduction
- 2 Methods
 - 2.1 Modeling Strategy
 - 2.2 Data
 - 2.2.1 In vitro / physico-chemical Data
 - 2.2.2 PK Data
 - 2.3 Model Parameters and Assumptions
 - 2.3.1 Absorption
 - 2.3.2 Distribution
 - 2.3.3 Metabolism and Elimination
 - 2.3.4 Tissue Concentrations
 - 2.3.5 Automated Parameter Identification
- 3 Results and Discussion
 - 3.1 Final input parameters
 - 3.2 Diagnostics Plots
 - 3.3 Concentration-Time Profiles
- 4 Conclusion
- 5 References

1 Introduction

Inulin is a highly hydrophilic polysaccharide which does not distribute into cells and is cleared via glomerular filtration.

Inulin has a considerably smaller solute radius than the proteins which had been used to develop the generic large molecule physiologically based pharmacokinetic (PBPK) model in PK-Sim ([Niederalt 2018](#)).

The herein presented evaluation report evaluates the performance of the PBPK model for inulin in rats using the large molecule model in PK-Sim.

The presented inulin PBPK model as well as the respective evaluation plan and evaluation report are provided open-source (<https://github.com/Open-Systems-Pharmacology/Inulin-Model>).

2 Methods

2.1 Modeling Strategy

The development of the large molecule PBPK model in PK-Sim® has previously been described by Niederalt et al. ([Niederalt 2018](#)). In short, the model was built as an extension of the PK-Sim® model for small molecules incorporating (i) the two-pore formalism for drug extravasation from blood plasma to interstitial space, (ii) lymph flow, (iii) endosomal clearance and (iv) protection from endosomal clearance by neonatal Fc receptor (FcRn) mediated recycling.

For model development and evaluation, PK data were used from compounds with a wide range of solute radii and from different species. The PK data used for parameter estimation were from the following compounds: antibody–drug conjugate BAY 79-4620 in mice (Bayer in house data), antibody 7E3 in wild-type and FcRn knockout mice ([Garg 2007](#), [Garg2009](#)), domain antibody dAb2 in mice ([Sepp 2015](#)), antibodies MEDI-524 and MEDI-524-YTE in monkeys ([Dall'Acqua 2006](#)), and antibody CDA1 in humans ([Taylor 2008](#)). The PK data used for model evaluation were from inulin in rats ([Tsuji1983](#)) and tefibazumab in humans ([Reilly 2005](#)).

The PBPK model including the estimated physiological parameters as described by Niederalt et al. ([Niederalt 2018](#)) is available in the Open Systems Pharmacology Suite from version 7.1 onwards.

This evaluation report focuses on the PBPK model for inulin.

Details about input data (physicochemical, *in vitro* and PK) can be found in [Section 2.2](#).

Details about the structural model and its parameters can be found in [Section 2.3](#).

2.2 Data

2.2.1 In vitro / physico-chemical Data

A literature search was performed to collect available information on physicochemical properties of Inulin. The obtained information from literature is summarized in the table below.

Parameter	Unit	Value	Source	Description
MW	g/mol	5000-5500	Ohno 1978	Molecular weight
r	nm	1.39	Ghandehari 1997	Hydrodynamic solute radius
logP	μ M	< -10	Dubbelboer 2022	Lipophilicity (octanol/water partition coefficient). Inulin is highly hydrophilic. A logP = -10 is insensitively small in the PBPK model.
Kd (FcRn)	μ M	999,999		Dissociation constant for binding to FcRn. High value representing no FcRn binding.

2.2.2 PK Data

Published plasma and tissue PK data on inulin in rats were used.

Publication	Description
Tsuji 1983	Plasma and tissue concentrations after i.v. application of 20 and 200 mg/kg inulin in rats (for 200 mg/kg plasma only).

2.3 Model Parameters and Assumptions

2.3.1 Absorption

There is no absorption process since inulin was administered intravenously

2.3.2 Distribution

The standard vascular properties of the different tissues (hydraulic conductivity, pore radii, fraction of flow via large pores) and standard lymph and fluid recirculation flow rates from PK-Sim were used ([Niederalt 2018](#)).

2.3.3 Metabolism and Elimination

Inulin is renally excreted via glomerular filtration. The standard glomerular filtration rate from the PK-Sim library was used (GFR fraction = 1).

2.3.4 Tissue Concentrations

For the comparison with experimental data the parameters `Fraction of blood for sampling` used in the Observer for the tissue concentrations were set for all organs to 0.18. This value is based on the parameter identification for different compounds reported in Ref. ([Niederalt 2018](#)) for comparison with tissue dissection data. (The parameter `Fraction of blood for sampling` specifies residual blood in tissue as ratio of blood volume contributing to the measured tissue concentration to the total in vivo capillary blood volume.)

Model Parameter	Value	Unit
Fraction of blood for sampling (all organs)	0.18	

Experimentally, gut concentrations (from duodenum to the cecum) were measured ([Tsuji 1983](#)). In the present evaluation report, the experimental gut concentrations were compared to simulated organ concentrations for small and large intestine separately in the goodness of fit plots as well as in the concentration-time profile plot.

2.3.5 Automated Parameter Identification

No drug specific parameters were fitted.

3 Results and Discussion

The PBPK model for inulin was evaluated with plasma and tissue PK data from rats.

The next sections show:

1. the final model parameters for the building blocks: [Section 3.1](#).
2. the overall goodness of fit: [Section 3.2](#).
3. simulated vs. observed concentration-time profiles for the clinical studies used for model building and for model verification: [Section 3.3](#).

3.1 Final input parameters

The compound parameter values of the final PBPK model are illustrated below.

Compound: Inulin

Parameters

Name	Value	Value Origin	Alternative	Default
Solubility at reference pH	9999 mg/l	Other-/Dummy value not used in the simulation	Measurement	True
Reference pH	7	Other-/Dummy value not used in the simulation	Measurement	True
Lipophilicity	-10 Log Units	Other-Highly hydrophilic	Measurement	True
Fraction unbound (plasma, reference value)	1	Other-Assumption	Measurement	True
Is small molecule	Yes			
Molecular weight	5500 g/mol	Publication-Ohno1978		
Plasma protein binding partner	Unknown			
Radius (solute)	0.00139 μm	Publication-Ghandehari1997		

Calculation methods

Name	Value
Partition coefficients	PK-Sim Standard
Cellular permeabilities	PK-Sim Standard

Processes

Systemic Process: Glomerular Filtration-GFR

Species: Human

Parameters

Name	Value	Value Origin
GFR fraction	1	Publication-Other-Tsuji1983 (DOI: 10.1002/jps.2600721103)

3.2 Diagnostics Plots

Below you find the goodness-of-fit visual diagnostic plots for the PBPK model performance of all data used presented in [Section 2.2.2](#).

The first plot shows observed versus simulated plasma concentration, the second weighted residuals versus time.

Table 3-1: GMFE for Goodness of fit plot for concentration in plasma and tissues

Group	GMFE
Plasma concentrations (20 & 200 mg/kg dose)	1.38
Tissue concentrations (20 mg/kg dose)	2.01
All	1.71

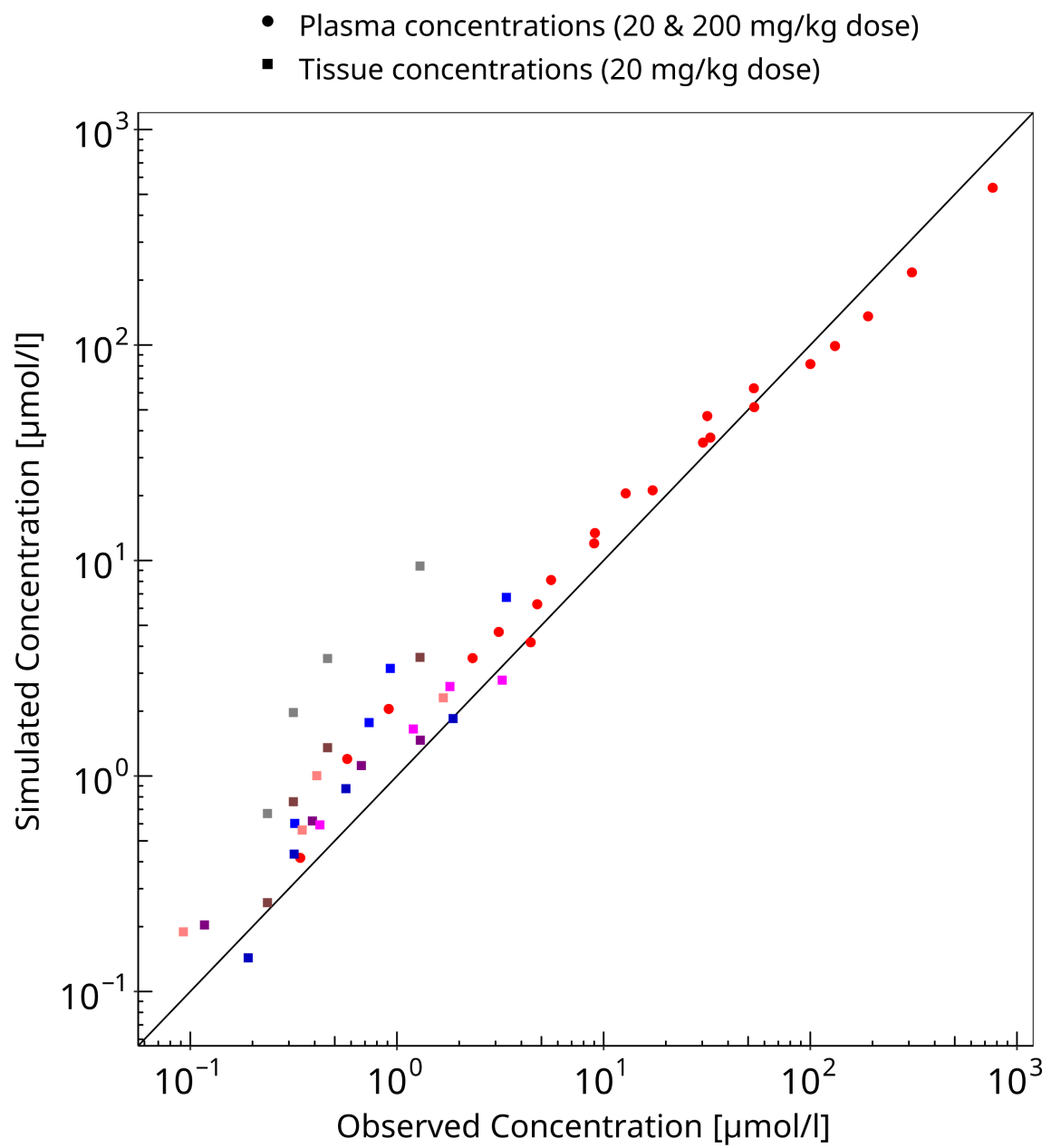


Figure 3-1: Goodness of fit plot for concentration in plasma and tissues

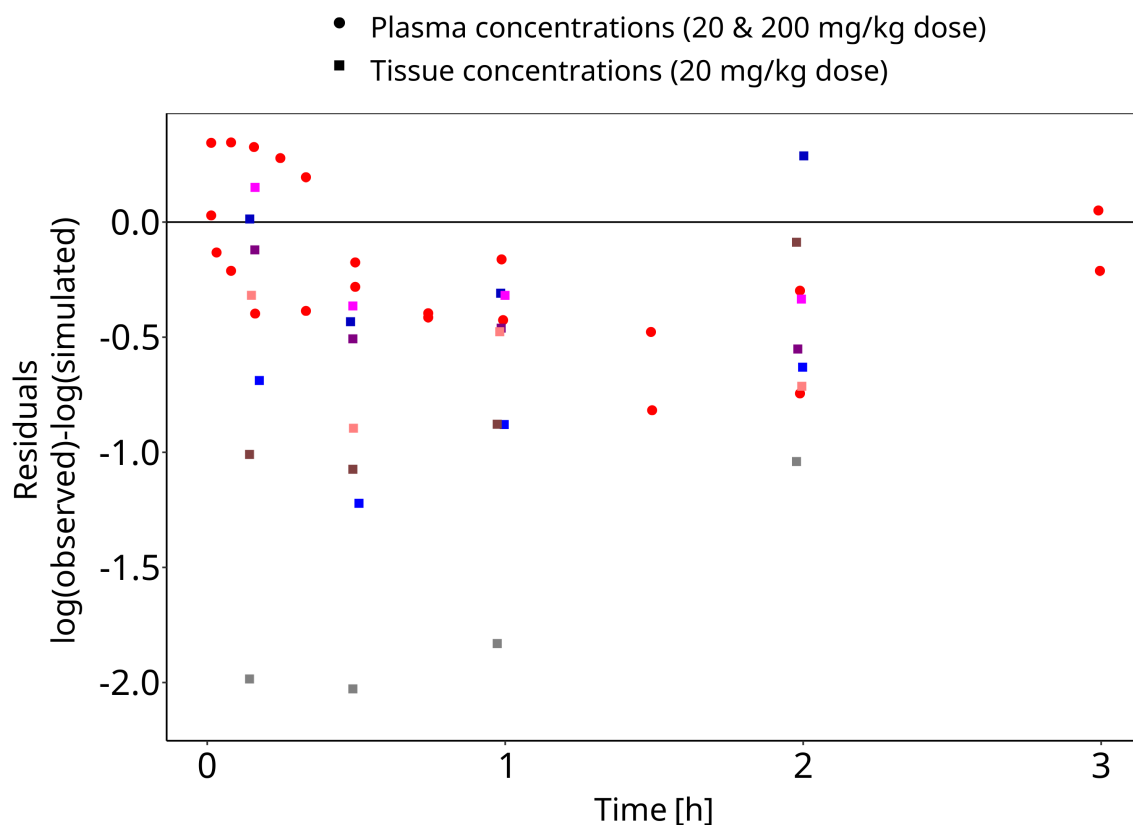


Figure 3-2: Goodness of fit plot for concentration in plasma and tissues

3.3 Concentration-Time Profiles

Simulated versus observed concentration-time profiles of all data listed in [Section 2.2.2](#) are presented below.

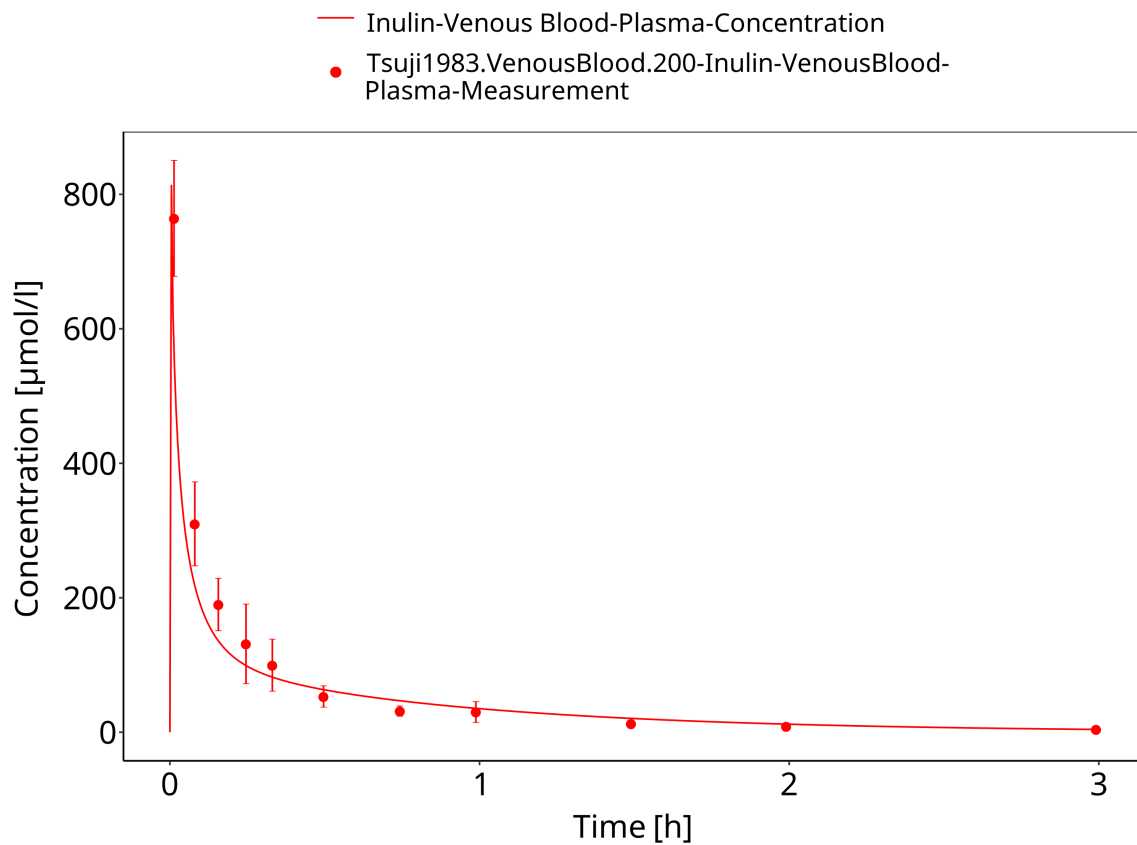


Figure 3-3: Plasma concentration (linear scale)

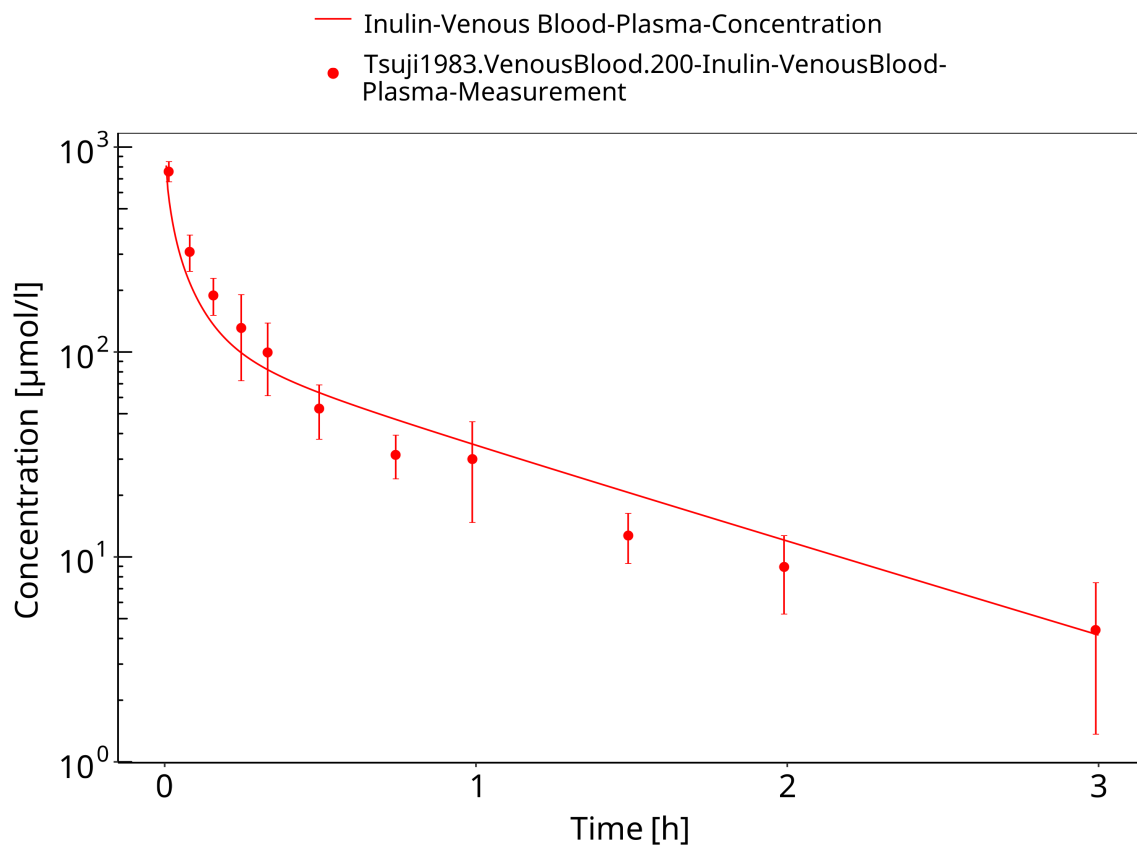


Figure 3-4: Plasma concentration (log scale)

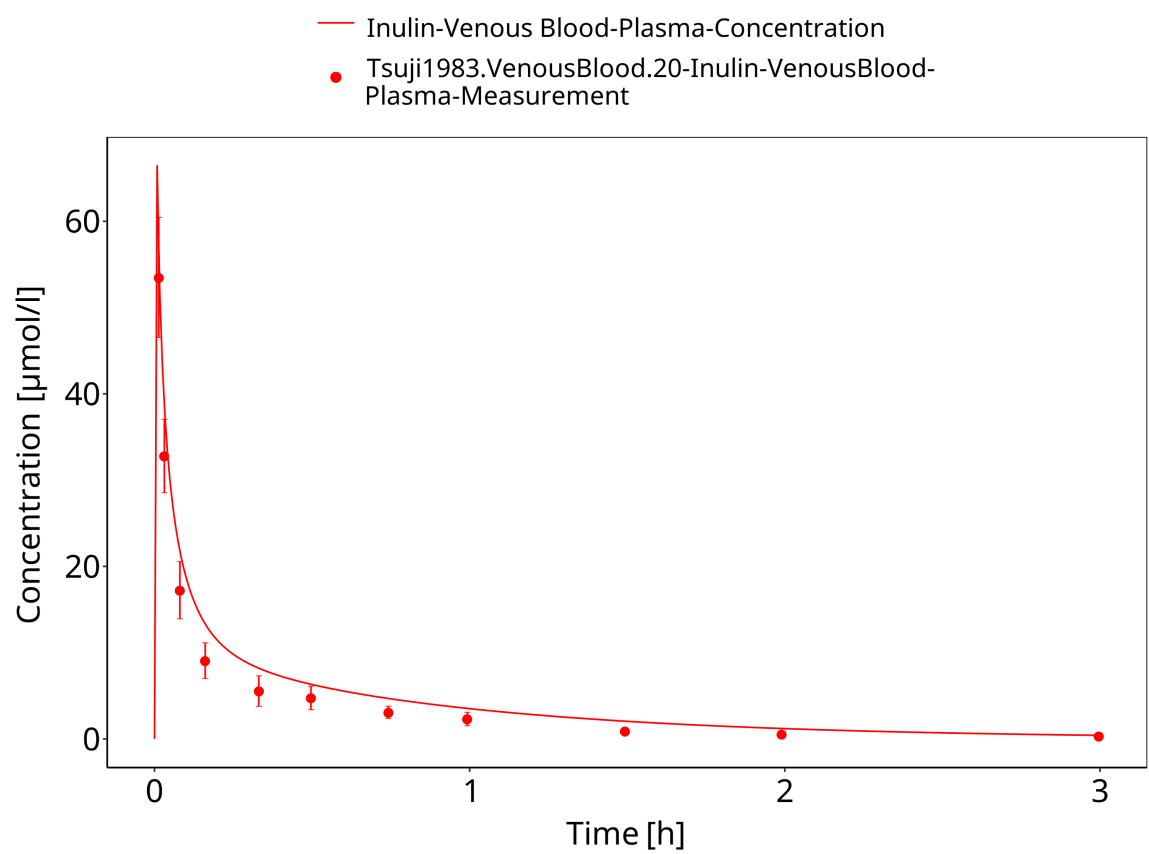


Figure 3-5: Plasma (linear scale)

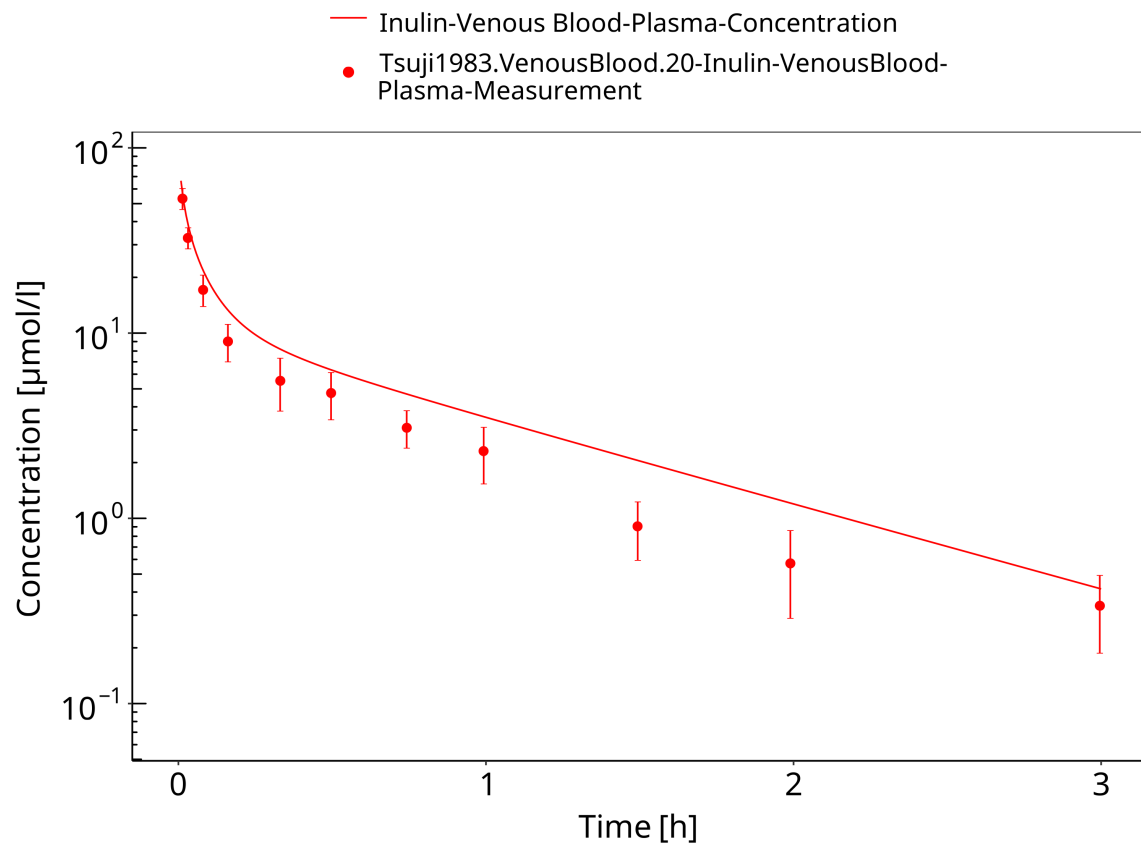


Figure 3-6: Plasma (log scale)

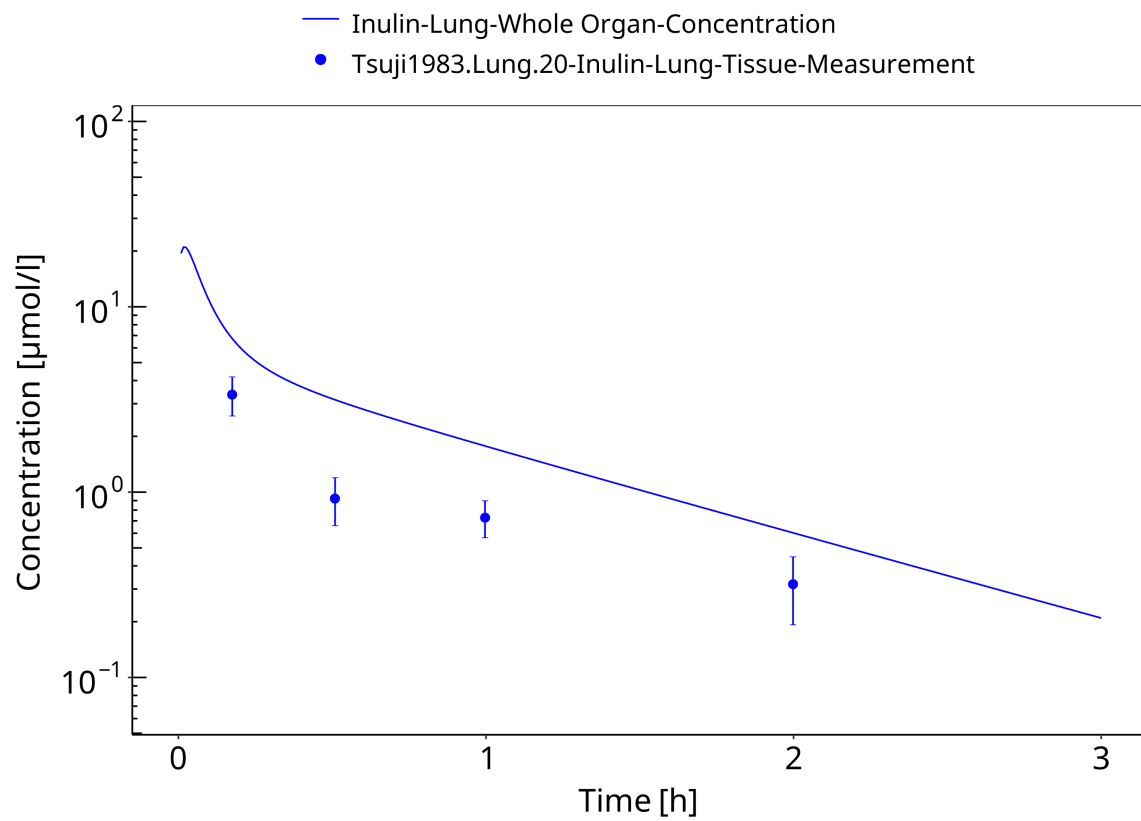


Figure 3-7: Lung

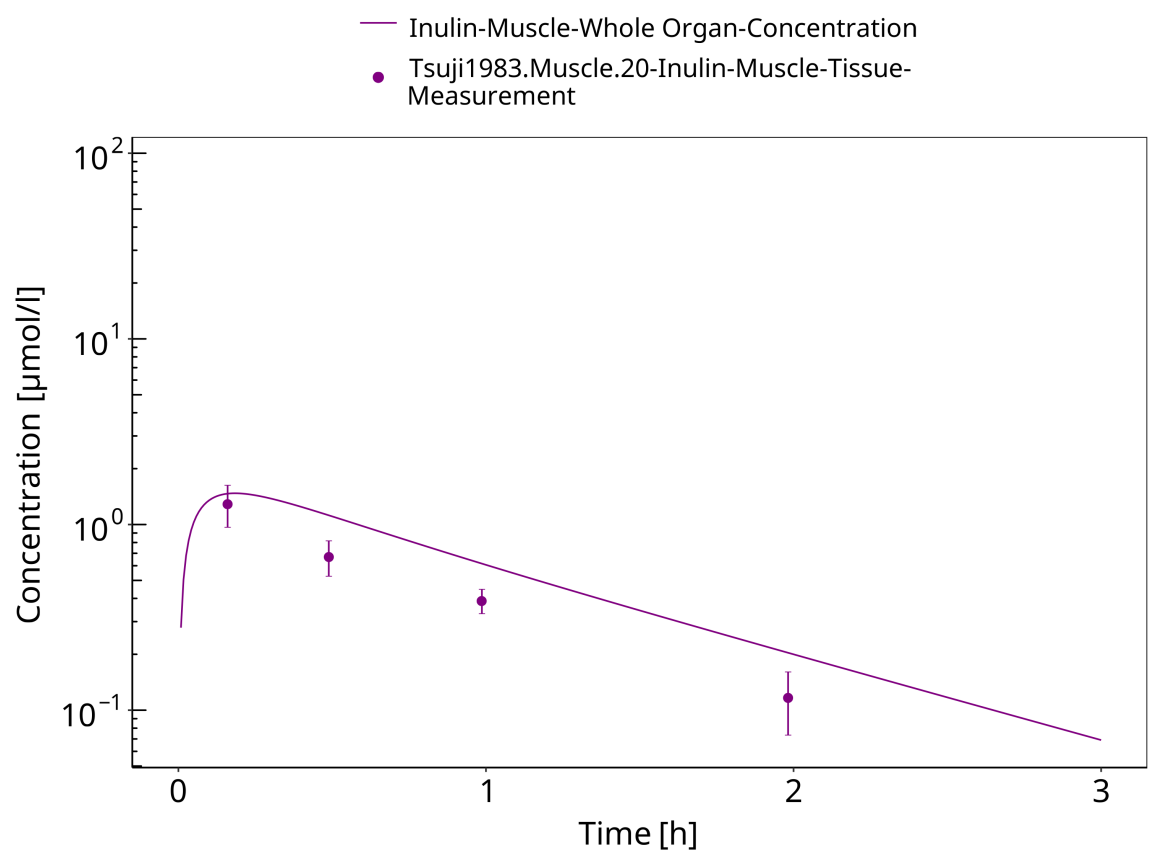


Figure 3-8: Muscle

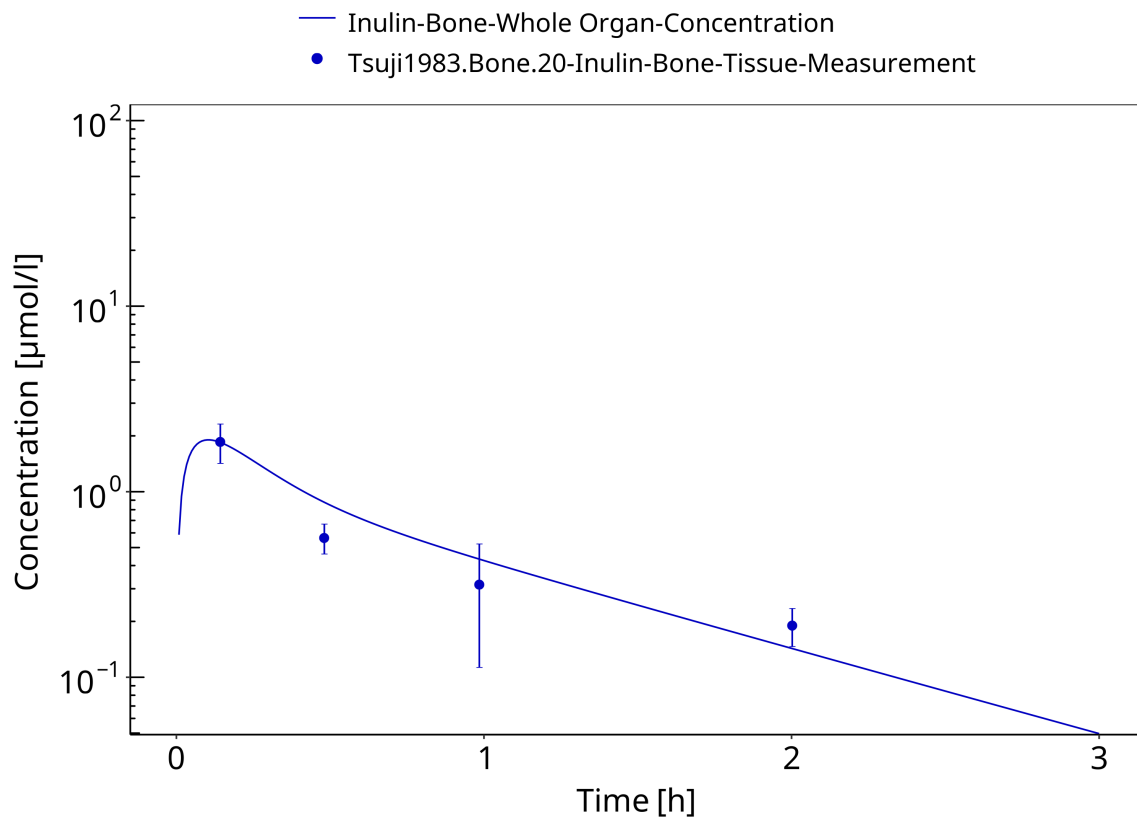


Figure 3-9: Bone

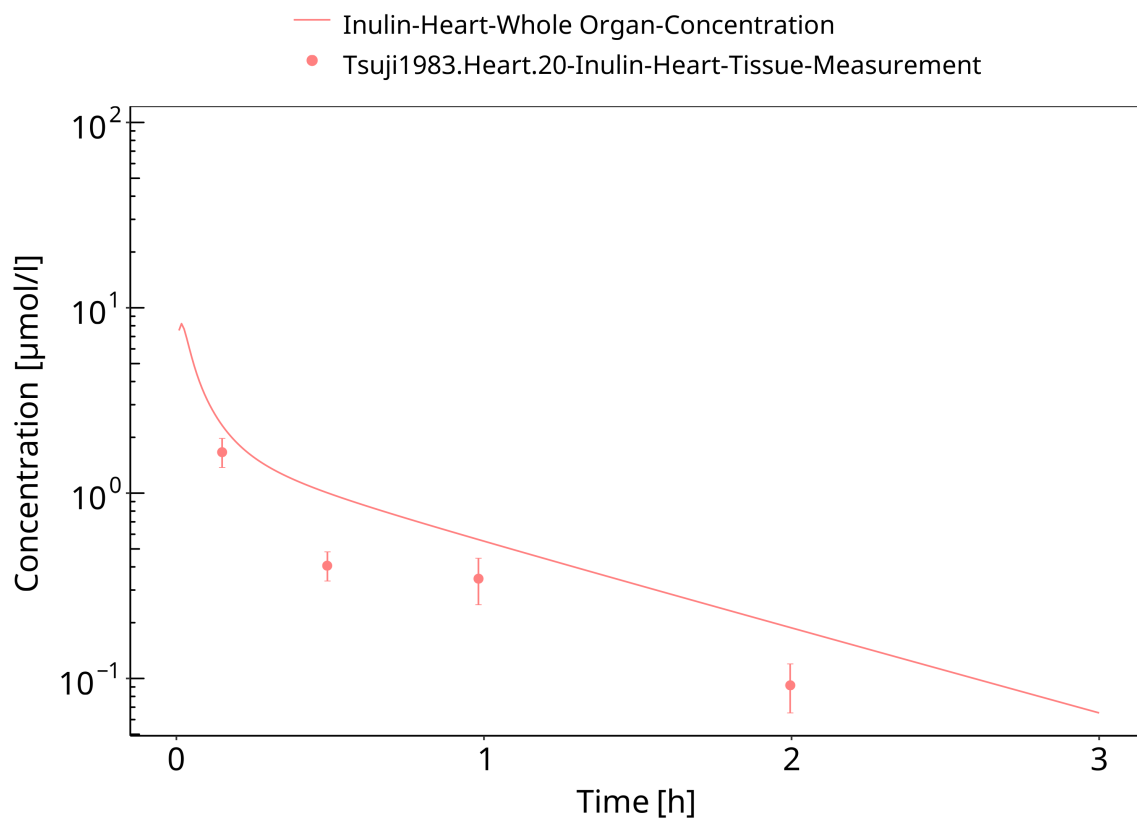


Figure 3-10: Heart

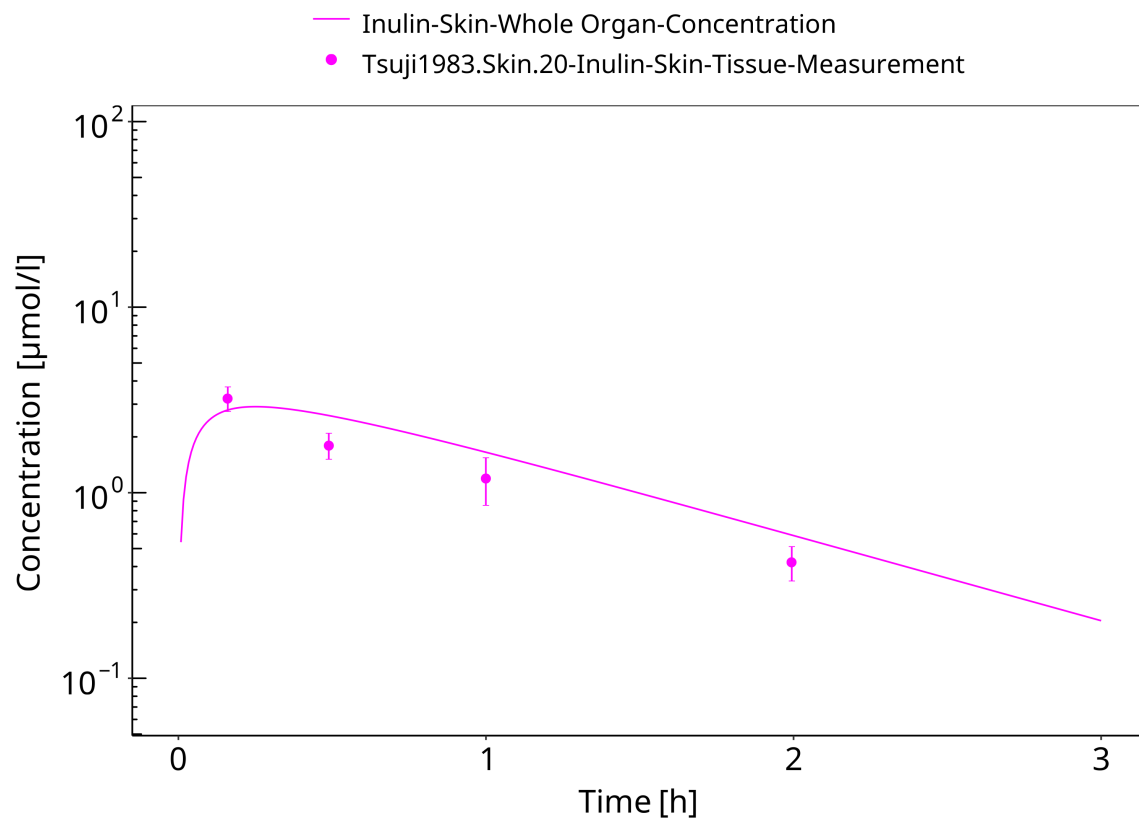


Figure 3-11: Skin

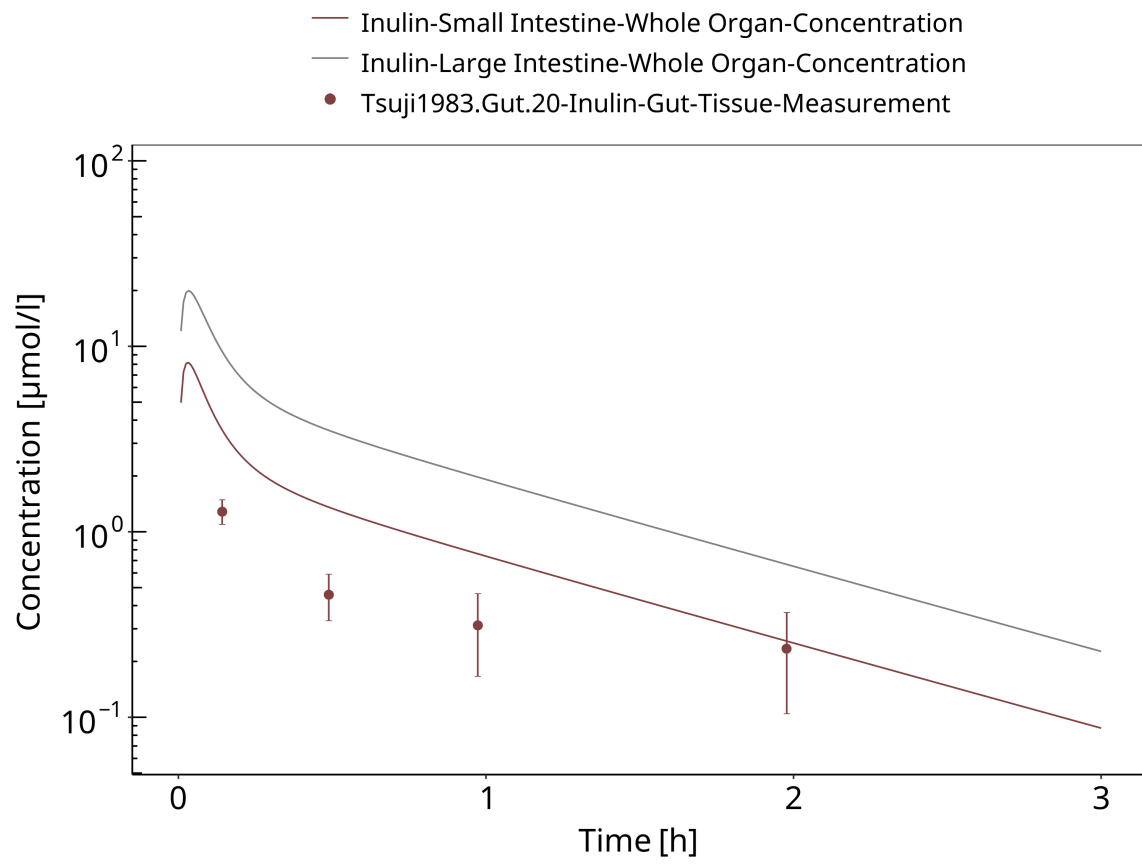


Figure 3-12: Gut

4 Conclusion

The herein presented PBPK model overall adequately describes the plasma pharmacokinetics of inulin in rats. Tissue concentrations tend to be overestimated by the model, the largest deviations being observed for lung, gut, and heart concentrations. Simulations are predictions without adjusting any compound specific parameter (i.e., using a literature value for the solute radius of inulin and the default physiological parameters in PK-Sim especially for the glomerular filtration rate, vascular properties and compartment volumes).

5 References

- Dall'Acqua 2006** Dall'Acqua WF, Kiener PA, Wu H. Properties of human IgG1s engineered for enhanced binding to the neonatal Fc receptor (FcRn). *J Biol Chem*. 2006 Aug; 281(33):23514-23524. doi: 10.1074/jbc.M604292200.
- Dubbelboer 2022** Dubbelboer, I. R., Sjögren, E. Overview of authorized drug products for subcutaneous administration: Pharmaceutical, therapeutic, and physicochemical properties. *European Journal of Pharmaceutical Sciences*. 2022 Jun; 173:106181. doi.org/10.1016/j.ejps.2022.106181.
- Garg 2007** Garg A, Balthasar JP. Physiologically-based pharmacokinetic (PBPK) model to predict IgG tissue kinetics in wild-type and FcRn-knockout mice. *J Pharmacokinet Pharmacodyn*. 2007 Jul; 34(5):687-709. doi: 10.1007/s10928-007-9065-1.
- Garg 2009** Garg A, Balthasar J. Investigation of the influence of FcRn on the distribution of IgG to the brain. *AAPS J*. 2009 July; 11(3):553-557. doi: 10.1208/s12248-009-9129-9.
- Ghandehari 1997** Ghandehari H, Smith PL, Ellens H, Yeh PY, Kopecek J. Size-dependent permeability of hydrophilic probes across rabbit colonic epithelium. *J Pharmacol Exp Ther*. 1997 Feb; 280(2):747-753.
- Lobo 2004** Lobo ED, Hansen R J, Balthasar JP. Antibody pharmacokinetics and pharmacodynamics. *J Pharm Sci*. 2004 Nov;93(11):2645-2668. doi: 10.1002/jps.20178.
- Niederalt 2018** Niederalt C, Kuepfer L, Solodenko J, Eissing T, Siegmund HU, Block M, Willmann S, Lippert J. A generic whole body physiologically based pharmacokinetic model for therapeutic proteins in PK-Sim. *J Pharmacokinet Pharmacodyn*. 2018 Apr;45(2):235-257. doi: 10.1007/s10928-017-9559-4.
- Ohno 1978** Ohno K, Pettigrew KD, Rapoport SI. Lower limits of cerebrovascular permeability to nonelectrolytes in the conscious rat. *American Journal of Physiology-Heart and Circulatory Physiology*. 1978 Sep;235(3):H299-H307. doi: 10.1152/ajpheart.1978.235.3.H299.
- Reilly 2005** Reilly S, Wenzel E, Reynolds L, Bennett B, Patti JM, Hetherington S. Open-label, dose escalation study of the safety and pharmacokinetic profile of tefibazumab in healthy volunteers. *Antimicrob Agents Chemother*. 2005 Mar;49(3):959–962. doi: 10.1128/AAC.49.3.959-962.2005.
- Sepp 2015** Sepp A, Berges A, Sanderson A, Meno-Tetang G. Development of a physiologically based pharmacokinetic model for a domain antibody in mice using the two-pore theory. *J Pharmacokinet Pharmacodyn*. 2015 Jan;42(2):97-109. doi: 10.1007/s10928-014-9402-0.
- Taylor 1984** Taylor AE, Granger DN. Exchange of macromolecules across the microcirculation. *Handbook of Physiology - Cardiovascular System. Microcirculation* (Eds. Renkin EM and Michel CC. Bethesda, MD, American Physiological Society). 1984; Vol. 4(Pt 2):467–520.
- Taylor 2008** Taylor CP, Tummala S, Molrine D, Davidson L, Farrell RJ, Lembo A, Hibberd PL, Lowy I, Kelly CP. Open-label, dose escalation phase I study in healthy volunteers to evaluate the safety and pharmacokinetics of a human monoclonal antibody to *Clostridium difficile* toxin A. *Vaccine*. 2008 Jun;26(27-28):3404–3409. doi: 10.1016/j.vaccine.2008.04.042.
- Tsuji 1983** Tsuji A, Yoshikawa T, Nishide K, Minami H, Kimura M, Nakashima E, Terasaki T, Miyamoto E, Nightingale CH, Yamana T. Physiologically based pharmacokinetic model for beta-lactam antibiotics I: tissue distribution and elimination in rats. *J Pharm Sci*. 1983 Nov;72(11):1239-1252. doi: 10.1002/jps.2600721103.

